Am J Physiol Heart Circ Physiol
280: H2804–H2814, 2001.

Sympathetic restraint of respiratory sinus arrhythmia: implications for vagal-cardiac tone assessment in humans

J. ANDREW TAYLOR, CHRISTOPHER W. MYERS, JOHN R. HALLIWILL, HENRIK SEIDEL, AND DWAIN L. ECKBERG
Departments of Internal Medicine and Physiology, Hunter Holmes McGuire Department of Veterans Affairs Medical Center, Richmond 23249; and Medical College of Virginia at Virginia Commonwealth University, Richmond, Virginia 23284

Received 25 July 2000; accepted in final form 14 February 2001

Taylor, J. Andrew, Christopher W. Myers, John R. Halliwill, Henrik Seidel, and Dwain L. Eckberg. Sympathetic restraint of respiratory sinus arrhythmia: implications for vagal-cardiac tone assessment in humans. *Am J Physiol Heart Circ Physiol* 280: H2804–H2814, 2001.—Clinicians and experimentalists routinely estimate vagal-cardiac nerve traffic from respiratory sinus arrhythmia. However, evidence suggests that sympathetic mechanisms may also modulate respiratory sinus arrhythmia. Our study examined modulation of respiratory sinus arrhythmia by sympathetic outflow. We measured R-R interval spectral power in 10 volunteers that breathed sequentially at 13 frequencies, from 15 to 3 breaths/min, before and after β-adrenergic blockade. We fitted changes of respiratory frequency R-R interval spectral power with a damped oscillator model: frequency-dependent oscillations with a resonant frequency, generated by driving forces and modified by damping influences. β-Adrenergic blockade enhanced respiratory sinus arrhythmia at all frequencies (at some, fourfold). The damped oscillator model fit experimental data well (39 of 40 ramps; $r = 0.86 \pm 0.02$). β-Adrenergic blockade increased respiratory sinus arrhythmia by amplifying respiration-related driving forces ($P < 0.05$), without altering resonant frequency or damping influences. Both spectral power data and the damped oscillator model indicate that cardiac sympathetic outflow markedly reduces heart period oscillations at all frequencies. This challenges the notion that respiratory sinus arrhythmia is mediated simply by vagal-cardiac nerve activity. These results have important implications for clinical and experimental estimation of human vagal cardiac tone.

autonomic nervous system; heart rate variability; vagus

HUMAN VAGAL-CARDIAC NERVE traffic has not been measured. Therefore, clinicians and experimentalists have been forced to rely on indirect methods to estimate the level of vagus nerve traffic to the heart. The use of respiratory sinus arrhythmia as a surrogate for vagal-cardiac nerve activity is supported by the highly linear relations that exist between vagus nerve traffic and respiratory sinus arrhythmia in spontaneously breathing anesthetized dogs (30) and between R-R intervals and respiratory sinus arrhythmia during progressive cholinergic blockade in humans (18, 47).

Although sympathetic-cardiac nerve activity fluctuates at respiratory frequencies (33, 34), oscillatory sympathetic stimuli do not provoke appreciable heart period responses at frequencies above ~0.15 Hz (4), probably because of the sluggishness of adrenergic receptor responses (23). The role of sympathetic activity in modulating respiratory-frequency heart period fluctuations is unclear. If "accentuated antagonism" (37) between sympathetic and vagal activities exists in humans, sympathetic nerve traffic should augment vagally induced heart period oscillations. If, on the other hand, cardiac sympathetic activity opposes vagal influences (21), sympathetic nerve activity should restrain vagally mediated heart period oscillations. In either case, estimates of vagal-cardiac nerve activity based on measurements of respiratory sinus arrhythmia may be confounded importantly by state and trait differences in sympathetic outflow, as, for example, in healthy subjects during postural changes (39) or in patients with cardiovascular diseases (1, 12, 44).

We tested the hypothesis that sympathetic nerve activity influences heart period oscillations over a wide range of breathing frequencies. We measured respiratory sinus arrhythmia in healthy young volunteers who breathed at frequencies between 15 and 3 breaths/min, before and after β-adrenergic blockade or combined β-adrenergic and muscarinic cholinergic blockade. For purposes of summarizing the data, we treated the amplitude relation of respiratory heart period fluctuations to breathing frequency as a damped oscillator, composed of frequency-dependent oscillations with a natural or resonant frequency, modified by driving forces and damping influences. Our analysis suggests that cardiac sympathetic nerve traffic reduces respiratory sinus arrhythmia by modulating driving force and thus restrains heart period oscillations at all frequencies. These findings challenge the notion that respiratory sinus arrhythmia is mediated simply by fluctuations of vagal-cardiac nerve traffic.

Address for reprint requests and other correspondence: J. A. Taylor, Laboratory for Cardiovascular Research, HRCA Research and Training Institute, 1200 Centre St., Boston, MA 02131 (E-mail: ataylor@mail.hrca.harvard.edu).

The costs of publication of this article were defrayed in part by the payment of page charges. The article must therefore be hereby marked "*advertisement*" in accordance with 18 U.S.C. Section 1734 solely to indicate this fact.

METHODS

Subjects. Ten healthy subjects (8 men and 2 women), 20–34 yr of age, participated in this study. The volunteers were nonsmokers without histories of cardiovascular or other major diseases and who were not taking medications. The subjects refrained from alcohol or caffeine ingestion and strenuous physical activity for 24 h preceding the study sessions.

This research was approved by the human research committees of the Hunter Holmes McGuire Department of Veterans Affairs Medical Center and the Medical College of Virginia at Virginia Commonwealth University. All of the volunteers gave their written informed consent to participate.

Measurements. We recorded electrocardiographic lead II, beat-by-beat finger photoplethysmographic arterial pressure (Finapres, Ohmeda), brachial arterial pressure (Dynamap, Critikon) every 3 min, respiratory excursions (pneumobelt), breath-by-breath tidal volume (Fleisch pneumotachograph), and end-tidal CO_2 concentrations (infrared analyzer connected to a mouthpiece with a two-way respiratory valve). We recorded all signals continuously on frequency modulation tape for subsequent analog-to-digital conversion.

We measured resting alveolar ventilation (V_A) at the beginning of each experiment with subjects in the 40° upright tilt position as the difference between minute ventilation and physiological dead space ventilation (V_D), calculated from end-tidal CO_2, mixed-expired CO_2, average expiratory volume, and breathing frequency according to the Bohr equation (9). Thus tidal volume (V_T) for each breathing frequency (f_B) was

$$V_T(\text{1/breath}) = V_D(\text{1/breath}) + [V_A(\text{1/min}) \div f_B(\text{breaths/min})] \quad (1)$$

Each experiment was composed of six sets of ramped frequency breathing, from 15 to 3 breaths/min (0.25–0.05 Hz), performed in sequential decrements of 1 breath/min for 96 s each (total time for one ramp of breathing: ~21 min). The measure of resting alveolar ventilation was used to calculate the tidal volume at each breathing frequency that would maintain alveolar ventilation constant. Subsequently, subjects controlled their breathing via visual feedback from an oscilloscope, which provided both frequency and volume for each inspiration. During each set of ramped breathing frequencies, subjects either increased tidal volume progressively as breathing slowed (constant alveolar ventilation) or maintained tidal volume at a constant high level, according to the largest tidal volume measured during increasing tidal breathing (i.e., at 3 breaths/min). We used constant tidal breathing to avoid the influence of differences in tidal volume on respiratory sinus arrhythmia (8). We bled a gas mixture of 90% CO_2-10% O_2 into the inspired side of a two-way respiratory valve to maintain constant and normal breath-by-breath end-tidal CO_2 levels. Thus, in our protocol, the subjects maintained adequate alveolar ventilation and normal end-tidal CO_2 regardless of breathing frequency or depth. More importantly, breathing frequency and volume did not vary between pharmacological blockade conditions.

Protocol. After the subjects underwent catheter insertion, instrumentation, and instruction, they rested supine for at least 10 min. They performed ramped frequency breathing after three intravenous injections given in a fixed order: saline (control), atenolol (0.2 mg/kg, β-adrenergic blockade), and atropine sulfate (0.04 mg/kg, combined β-adrenergic and muscarinic cholinergic blockade). We gave injections to the subjects as they lay in the supine position, allowed a 7-min drug effect period, and then tilted subjects to 40°. All experimental measurements were made with the subjects tilted. We used tilt to increase sympathetic neural outflow, because healthy young humans have low levels of sympathetic outflow in the supine position (58). We made recordings 3 min after 40° tilt, during decreasing frequency breathing, with increasing tidal volume and with constant tidal breathing, performed in random order. Subjects rested for 10 min in the supine position between each pair of breathing ramps.

Data analysis. We digitized all data at 1,000 Hz with commercial computer hardware and software (Codas, Dataq Instruments), identified electrocardiographic R waves and arterial pressure peaks and valleys, and calculated means ± SE.

We performed fast Fourier transform analysis on beat-by-beat R-R intervals and systolic pressures as follows. Each 1,248-s time series of R-R intervals and arterial pressures was interpolated by a cubic spline function at 4 Hz to obtain equidistant time intervals. Data sets of 64 s (256 samples) overlapping by 32 s were detrended, Hanning filtered, and fast Fourier transformed to their frequency representation squared. Two periodograms were averaged to produce the spectrum estimate for each of 13 breathing frequencies (60). This procedure yielded spectral estimates, allowing detection of oscillations as slow as 0.05 Hz, the lowest breathing frequency studied. We integrated the area under the power spectrum at each breathing frequency (±0.02 Hz) for modeling and statistical comparisons. In what follows, we refer to R-R interval spectral power at the respiratory frequency as "respiratory sinus arrhythmia."

For the analysis of our data, we assumed that respiratory sinus arrhythmia after combined adrenergic and cholinergic blockade reflects the influence of mechanical stretch on the sinoatrial node, concurrent with respiration (52). Therefore, we subtracted spectral power measured after combined blockade from spectral power measured after saline and β-adrenergic blockade to obtain estimates of sinus arrhythmia with all autonomic components intact and with only vagal components intact.

Damped oscillator model. Figure 1 illustrates the spectral power of a damped oscillator at frequencies from 0.25 to 0.05 Hz, at three levels of forcing, and at three levels of damping. Maximum amplitude oscillations occur at the resonant frequency of the oscillator of 0.10 Hz. Both increased forcing with constant damping (Fig. 1*A*) and decreased damping with constant forcing (Fig. 1*B*) augment frequency domain measures of the oscillations. However, there are important differences in the impact of damping and forcing on the oscillations. Changes in driving force produce proportional changes of power at all frequencies, whereas changes of damping produce disproportionately greater changes in power at the resonant frequency than at other frequencies. The most profound differences are found at frequencies distant from the resonant frequency (see Fig. 1, *insets*). Proportional changes of power occur with different driving forces, but only small changes occur with different damping levels. We used the damped oscillator model to reduce respiratory spectral power during each breathing ramp to three terms, two of which have disparate effects across the frequency range examined.

The damped harmonic oscillator is driven by a cosinusoidal forcing function at the respiratory frequency. The steady-state behavior of such a system is described by a cosine oscillating at the respiratory frequency f_B. At time t, the R-R interval $x(t)$ of the oscillator is given by

$$x(t) = \frac{A}{\sqrt{(f_B^2 - c^2)^2 + (bf_B)^2}} \cos(f_B t - \phi) \quad (2)$$

where $\phi = \tan^{-1}[bf_B/(f_B{}^2 - c^2)]$ represents a phase shift between respiration and R-R interval and $J = A/\sqrt{b^2 f^2} +$

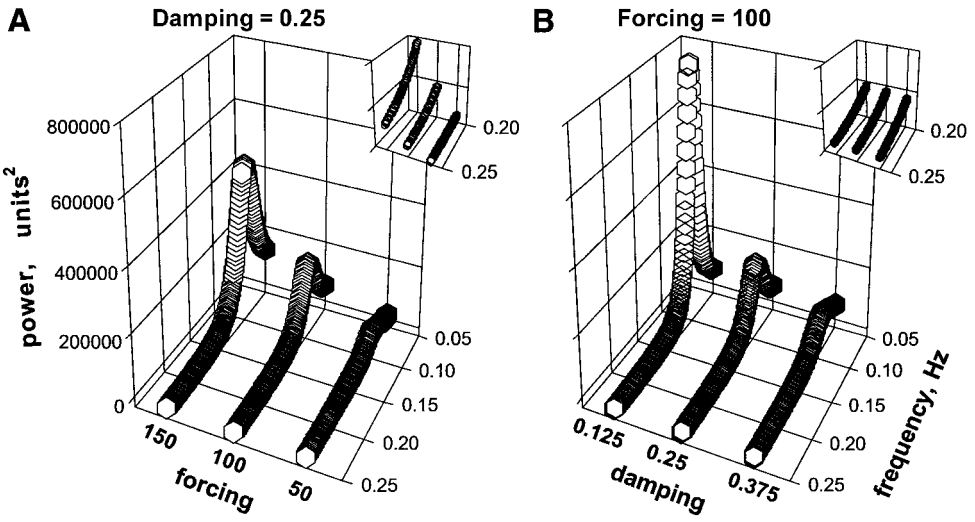

Fig. 1. Examples of power spectral data derived from the damped oscillator model at a 0.10-Hz resonant frequency with damping fixed and forcing varied (*A*) and with forcing fixed and damping varied (*B*). *Insets*: disparate effects of damping and forcing away from the resonant frequency.

$(f^2 - c^2)^2$ determines the amplitude of the R-R interval oscillations. The power spectrum of the time-domain signal given by *Eq. 2* is an impulse at frequency f_B with amplitude $P = J^2/2$. In *Eq. 2*, parameter A describes the strength of the driving force, b measures the influence of damping on the oscillator, and c represents the characteristic or resonant frequency of the oscillator. The amplitude of the oscillations is greatest when the frequency of the driving force approaches the resonant frequency of the oscillator, that is, when $f \approx c$.

Following the experimental protocol, breathing frequency, f_B in *Eq. 2,* decreased from 0.25 to 0.05 Hz in steps of 0.017 Hz every 96 s. To optimize the fits, we minimized the χ^2 error between P and the power estimated at each frequency. We did this by applying the Nelder-Mean simplex algorithm for ≥500 iterations with random initial parameter estimates drawn from a uniform distribution. This insures a high probability of finding the global minimum (46). We added a regularization term to the χ^2 error function to constrain the resonant frequency c of the oscillator to lie in the observable range of ≤0.25 Hz.

Statistical analysis. We measured the level of end-tidal CO_2 to assess the effectiveness of our subjects' control of tidal volume in maintaining alveolar ventilation during increasing tidal breathing and the effectiveness of our own manually increased levels of inspired CO_2 concentrations in preventing hypocapnia during constant (large) tidal breathing. We performed linear regression of 1-min averages to describe changes of end-tidal CO_2 over time and across breathing frequencies. We evaluated the effects of each drug and breathing condition on average R-R intervals and arterial pressures with repeated measures analysis of variance with a Bonferroni post hoc correction to identify significant differences. Spectral powers of R-R interval and systolic pressure variabilities were summarized by four variables: the average power across all breathing frequencies, the maximum power across all breathing frequencies, the minimum power across all breathing frequencies, and the power at 0.25 Hz breathing. Spectral powers were not distributed normally, even after log transformation, and model parameters also were not distributed normally. Therefore, we used a nonparametric Friedman repeated-measures analysis of variance on ranks to examine the effects of drug and breathing conditions. Significance was set at the $P < 0.05$. Data are reported as means ± SE.

RESULTS

Figure 2 depicts a sliding fast Fourier transform analysis of respiration, systolic pressure, and R-R intervals from one subject during progressive decreases of breathing frequency. In this example, increasing spectral power during decreasing breathing frequency reflects in part increasing tidal volumes (to maintain alveolar ventilation constant). These analyses document a strong influence of breathing rate on systolic pressure and R-R intervals.

The subjects controlled both breathing frequencies and tidal volumes very well. Across all subjects, the average standard deviation from target breathing frequency within each trial ranged from 0.008 to 0.018 Hz. In most subjects, the deviation was greatest during double-blockade trials (0.012 ± 0.001 Hz). During increasing tidal breathing, minimal changes in average end-tidal CO_2 indicate that alveolar ventilation was maintained constant, and thus volume was well controlled. When subjects breathed from faster to slower rates with increasing tidal volume, end-tidal CO_2 increased 0.009 ± 0.004% per minute (a net change of ~0.21% over the 21-min breathing protocol). Because we bled CO_2 into the breathing line during constant large tidal breathing, average end-tidal CO_2 increased slightly less (0.007 ± 0.007% per minute, a net increase of ~ 0.17%) but provides no indication of adequate volume control. However, the deviation from target volume was small. The average standard deviation from target volume within each constant tidal breathing trial ranged from 2.7 to 9.8% and, as with breathing frequency, tended to be greater during double blockade trials (6.0 ± 0.8%). Thus our subjects were able to precisely perform decreasing frequency breathing with either increasing or constant tidal volume. Moreover, an earlier study (22) suggests that the small changes of end-tidal CO_2 probably exerted no influence on our results.

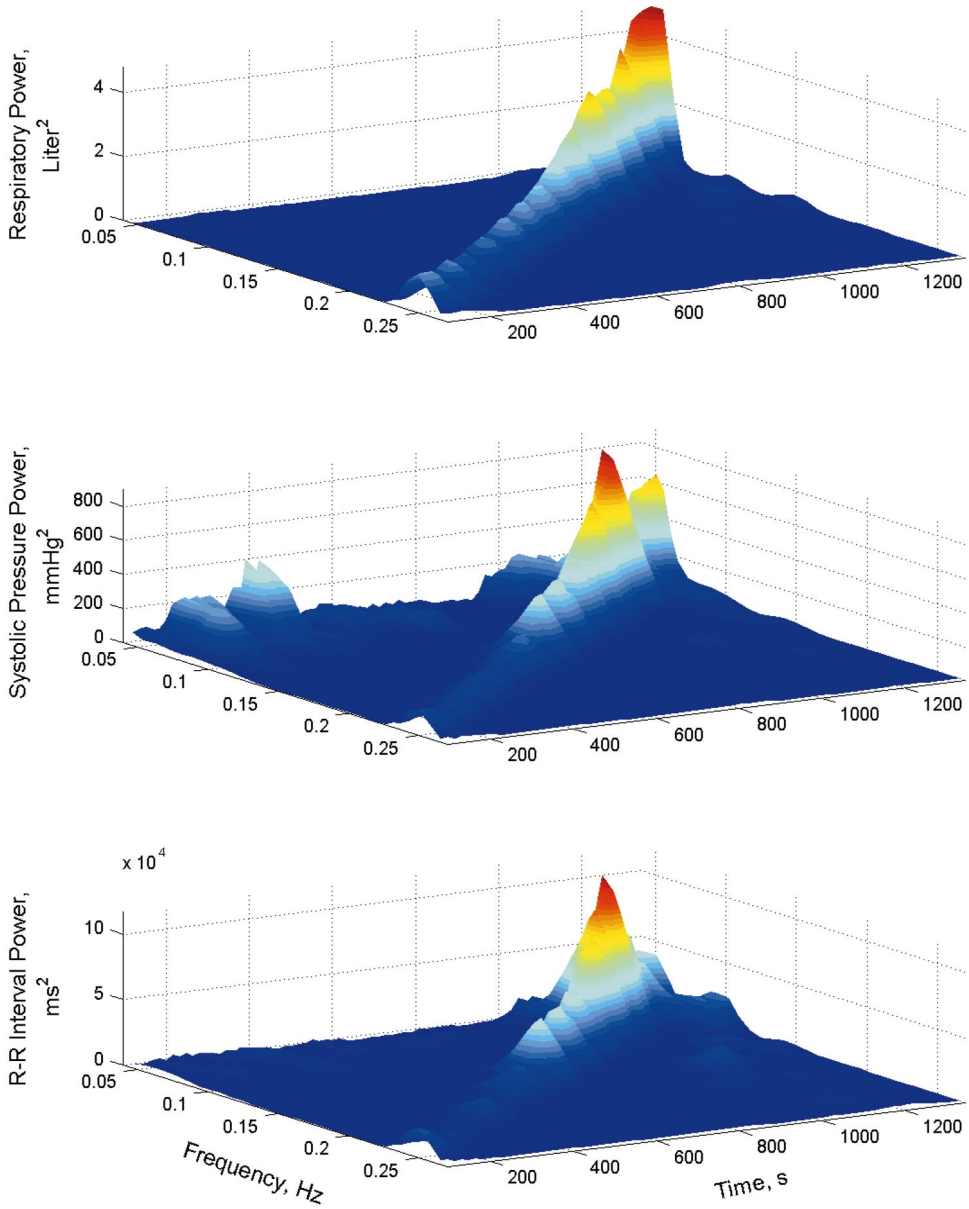

Fig. 2. Power spectral data for 1 subject during 21 min of decreasing frequency, increasing tidal breathing in the control condition.

Average hemodynamic values. Table 1 lists average hemodynamic measurements after saline, β-adrenergic blockade, and double autonomic blockade, with increasing or constant large tidal breathing. As expected, β-adrenergic blockade lengthened, and double autonomic blockade shortened average R-R intervals. Although double autonomic blockade tended to increase arterial pressure, only diastolic pressure during constant tidal breathing increased significantly. There were no significant differences in average hemodynamic values between breathing conditions, with one exception: R-R intervals after double autonomic block-

Table 1. *Average R-R intervals and arterial pressures across all frequencies for each drug and breathing condition*

	Control		β-Blockade		Double Blockade	
	Increasing V_T	Constant V_T	Increasing V_T	Constant V_T	Increasing V_T	Constant V_T
R-R interval, ms	866 ± 39	842 ± 32	1,040 ± 43*	1,012 ± 51*	706 ± 24*	673 ± 28*†
Systolic pressure, mmHg	127 ± 3	128 ± 4	120 ± 6	124 ± 5	130 ± 4	135 ± 3
Diastolic pressure, mmHg	71 ± 2	71 ± 2	66 ± 3	71 ± 3	76 ± 3	80 ± 3*

Values are means ± SE. V_T, tidal volume. *$P < 0.05$ vs. control, within breathing condition. †$P < 0.05$ vs. increasing V_T, within drug condition.

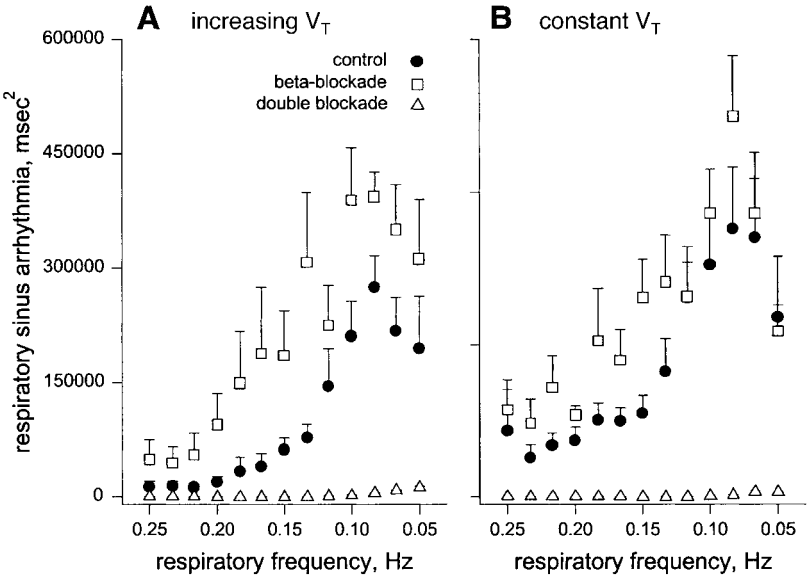

Fig. 3. Average respiratory sinus arrhythmia across all breathing frequencies with increasing tidal volume (V_T) (*A*) and constant tidal volume (*B*) during control, β-blockade, and double autonomic blockade conditions.

ade were larger during increasing than constant tidal breathing.

Arterial pressure variability. Systolic pressure oscillations tracked respiratory frequency and, as expected, were greatest at the slowest breathing frequencies and highest tidal volumes. Neither β-adrenergic blockade nor double autonomic blockade affected the average or the maximum systolic pressure spectral power across breathing frequencies. However, minimum systolic pressure spectral power and the systolic pressure spectral power during breathing at 0.25 Hz were less before autonomic blockade than after both β-adrenergic and double autonomic blockade with increasing tidal breathing. Constant tidal breathing increased all spectral indexes of respiratory frequency systolic pressure oscillations except maximal power when compared with increasing tidal breathing. This probably reflects the fact that maximum tidal volume was the same during the two breathing protocols.

Respiratory sinus arrhythmia. Figure 3 shows average respiratory sinus arrhythmia during control measurements and after β-adrenergic and double autonomic blockade, with increasing and constant tidal volumes. β-Adrenergic blockade enhanced respiratory sinus arrhythmia at all frequencies, at some breathing frequencies by a factor of 4. Conversely, double autonomic blockade reduced respiratory sinus arrhythmia at all frequencies, to <5% of control levels. Table 2 lists average indexes of respiratory sinus arrhythmia under all experimental conditions. β-Adrenergic and double autonomic blockade markedly affected all of these measures.

Respiratory sinus arrhythmia persisted despite major reduction after double autonomic blockade and achieved considerable amplitude at slow breathing frequencies. Figure 4 illustrates this in a representative subject. In this subject, R-R interval spectral power at slow breathing frequencies (0.05 Hz) after double autonomic blockade (Fig. 4*B*) exceeded spectral power at faster breathing frequencies (0.25 Hz) before autonomic blockade (Fig. 4*A*). In fact, maximum spectral power after double autonomic blockade was as great or greater than minimal respiratory sinus arrhythmia before autonomic blockade during both breathing protocols.

Table 2 also documents the influence of tidal volume changes during decreasing frequency breathing. Before β-adrenergic blockade, average, maximum, and minimum respiratory sinus arrhythmia, and spectral power at 0.25-Hz breathing, were significantly larger when tidal volume was large and constant than when it was steadily increasing. Constant large tidal breathing in-

Table 2. *Spectral power indexes of respiratory sinus arrhythmia for each drug and breathing condition*

	Control		β-Blockade		Double Blockade	
	Increasing V_T	Constant V_T	Increasing V_T	Constant V_T	Increasing V_T	Constant V_T
0.25 Hz power, ms^2	13,392 ± 7,643	86,398 ± 55,362†	49,499 ± 25,361†	114,750 ± 39,630*†	444 ± 210*	543 ± 152*
Average power, ms^2	101,199 ± 23,230	172,577 ± 36,566†	211,354 ± 41,364*	239,671 ± 39,834*	2,413 ± 286*	1,492 ± 176*†
Maximum power, ms^2	327,722 ± 54,260	434,179 ± 74,969†	558,873 ± 78,563*	564,921 ± 81,539*	13,587 ± 1,921*	7,937 ± 1,596*†
Minimum power, ms^2	8,508 ± 4,019	29,218 ± 7,242†	34,171 ± 16,399*	53,894 ± 12,341*†	197 ± 125*	122 ± 45*

Values are means ± SE. *$P < 0.05$ vs. control, within breathing condition. †$P < 0.05$ vs. increasing V_T, within drug condition.

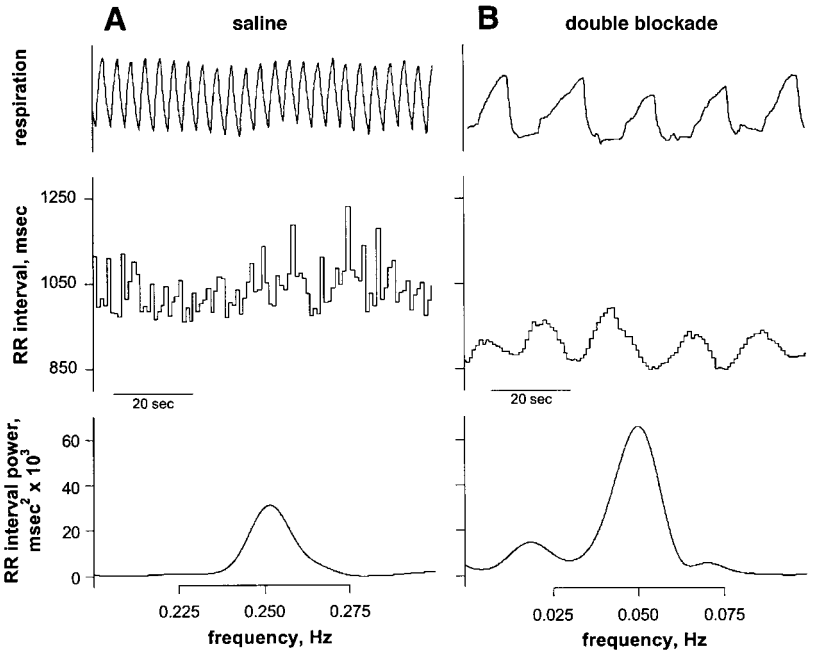

Fig. 4. Example from 1 subject, documenting comparable respiratory sinus arrhythmia at a slow breathing frequency (0.05 Hz) during double autonomic blockade (*B*) and standard breathing frequency (0.25 Hz) during control conditions (saline; *A*). Tidal volumes are the same. Although spectral power was much lower after double autonomic blockade than during control conditions, significant fluctuations were still present.

creased respiratory sinus arrhythmia under most conditions.

Damped oscillator model. As described in METHODS, we attempted to remove the mechanical effects of respiration by subtracting respiratory sinus arrhythmia after double autonomic blockade from that measured before autonomic blockade and after β-adrenergic blockade. This paradigm allowed us to calculate coefficients for the damped oscillator model of respiratory sinus arrhythmia for two purely autonomic conditions: sympathetic and parasympathetic influences intact and sympathetic influences removed. Figure 5 shows a representative R-R interval time series from one subject with increasing tidal breathing (Fig. 5, *top*), a time series derived from the damped oscillator model treatment of the same data (Fig. 5, *middle*), and actual R-R interval spectral power derived from the R-R interval time series (circles) and the damped oscillator model (Fig. 5, *bottom*). The damped oscillator model provided an excellent fit to the measured spectral power and generated a good representation of the original time series (Fig. 5, *middle*).

The damped oscillator model provided an adequate ($r \geq 0.70$) fit for all but one of the 40 data series; the correlation coefficients for the other 39 data series averaged 0.86 ± 0.02. Figure 6 depicts average damped oscillator coefficients (see *Eq. 2*) under all conditions. Out of the three parameters derived from the damped oscillator model, only the resonant frequency (*c*) was unchanged by β-adrenergic blockade or breathing condition. Resonant frequencies averaged 0.081 ± 0.005 Hz and ranged from 0.073 (β-adrenergic blockade, constant tidal volume) to 0.092 Hz (β-adrenergic blockade, increasing tidal volume). According to the model, β-adrenergic blockade increased respiratory sinus arrhythmia by increasing respiration-related driving forces (*A* in *Eq. 2*) for respiratory sinus arrhythmia ($P < 0.05$,

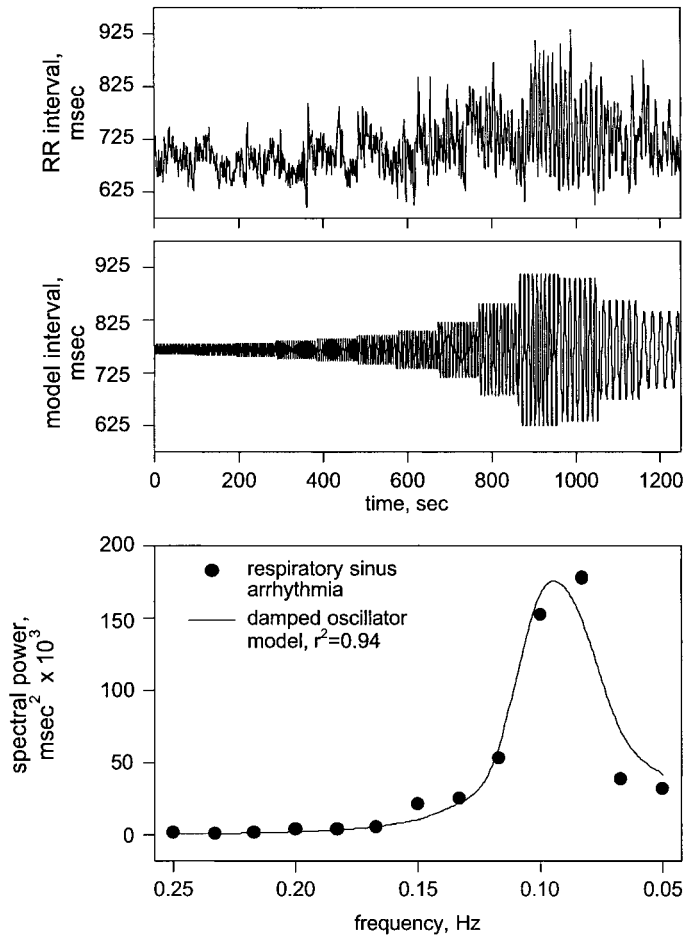

Fig. 5. R-R interval time series during decreasing frequency, increasing tidal breathing (*top*), the time series derived from the damped oscillator model of this time series (*middle*), and the measured respiration-related R-R interval spectral power (●) and the damped oscillator model (*bottom*).

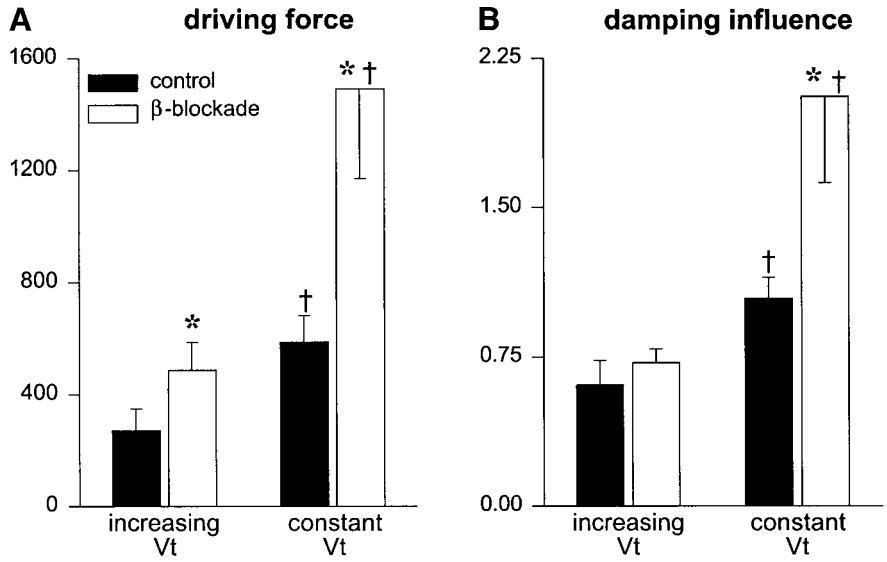

Fig. 6. Driving force (*A*) and damping influence (*B*) for respiratory sinus arrhythmia during increasing and constant tidal breathing under control and β-blockade conditions. Resonant frequency was unchanged by breathing or sympathetic blockade. *$P < 0.05$ vs. control within breathing condition. †$P < 0.05$ vs. increasing tidal volume within autonomic condition.

Fig. 6*A*). The calculated driving force was ~80% greater after β-adrenergic blockade with increasing tidal breathing, and more than 150% greater after β-adrenergic blockade with constant tidal breathing. Increased driving force in the absence of consistent changes of damping indicates that removal of cardiac sympathetic stimulation augments respiratory sinus arrhythmia in a nonfrequency-dependent manner.

Constant tidal breathing augmented respiratory sinus arrhythmia by increasing both driving force and damping ($P < 0.05$, Fig. 6*B*), effects that were augmented by β-adrenergic blockade. Increased driving force accompanied by greater damping indicates that large tidal breathing augments respiratory sinus arrhythmia at all breathing frequencies but has its greatest impact at frequencies higher than the resonant frequency.

DISCUSSION

We used a damped oscillator model to study the influence of breathing frequency and depth on respiratory sinus arrhythmia amplitude in healthy young men and women studied before and after autonomic blockade. Our results yielded several new insights. First, the damped oscillator model describes responses well and indicates that, although slow breathing increases respiratory sinus arrhythmia, very slow breathing reduces respiratory sinus arrhythmia to low levels. Second, sympathetic neural outflow restricts respiratory sinus arrhythmia at rapid as well as slow breathing frequencies. Therefore, respiratory sinus arrhythmia cannot be considered a purely vagal phenomenon. Third, phasic atrial stretch provokes major respiratory sinus arrhythmia at slow breathing frequencies.

Relation between breathing frequency and respiratory sinus arrhythmia. There is a substantial literature that indicates that slow breathing increases respiratory sinus arrhythmia (8, 19, 24). A study from our laboratory (10) showed that slow breathing might increase respiratory frequency R-R interval spectral power as much as 10-fold. In the present study, we confirm these earlier observations and extend them by showing that very slow breathing reduces respiratory sinus arrhythmia. This finding confirms observations made originally by Angelone and Coulter (2) and Womack (62), who used similar protocols, and by Saul and co-workers (51), who used a random ("white noise") frequency breathing protocol. Saul et al.'s (52) work showed that the phase relation between respiratory sinus arrhythmia and breathing shifts from a short lead to a long lag in the frequency range we examined. This agrees with the postulate that R-R interval shortening begins progressively further from end expiration as respiratory frequency declines, but that inspiration is always associated with R-R interval shortening (13). On the basis of his findings, Saul and co-workers (51) concluded that inspiratory gating of vagal-cardiac motoneuron firing is relatively broad pass with a corner frequency approaching the highest breathing rate we examined.

Because average R-R intervals were constant across all breathing frequencies in our study, mean vagal-cardiac nerve activity probably was also constant. If this inference is correct, the profound effect of breathing frequency on R-R interval fluctuations reflects primarily the kinetics of acetylcholine influences on the sinoatrial node. We speculate that during rapid breathing, there is less acetylcholine released during the expiratory phase (because it is of shorter duration). Because the time required for hydrolysis of acetylcholine is ~1.5–2.0 s (3, 16), responses to acetylcholine released during one expiration merge with responses to acetylcholine released during the next expiration. At slow, "resonant," breathing frequencies (see Fig. 3), more acetylcholine is released during expiration (because it is of longer duration), and, because of the time constants of acetylcholine hydrolysis, sinoatrial responses summate and maximally inhibit sinoatrial node firing.

Although we are not certain why very slow breathing reduces respiratory sinus arrhythmia, we offer two possible mechanisms. Respiratory sinus arrhythmia reflects intrinsic properties of the respiratory "gate" (38). Earlier research shows that the level of respiratory gating is a continuous function that varies sinusoidally during quiet breathing: the "gate" is not simply closed during inspiration and open during expiration (17). In fact, vagal responsiveness to arterial baroreceptor stimuli declines steadily during expiration (17). Therefore, during very slow breathing, when expiration is of very long duration, vagal-cardiac motoneurons may become relatively unresponsive to baroreceptor stimulation. Moreover, studies in animals (54) and humans (4, 14) indicate clearly that vagal responses to baroreceptor stimuli are not unidirectional: after brief baroreceptor stimuli, R-R intervals prolong and then shorten. It is conceivable that during long expiratory pauses, as gating of new baroreceptor stimulation of vagal-cardiac motoneuron increases, R-R interval shortening occurs, unopposed.

Autonomic mediation of respiratory sinus arrhythmia. The view of respiratory sinus arrhythmia as a purely vagal phenomenon is widely held and is supported by substantial published data. In dogs, vagal-cardiac nerve traffic has a distinct respiratory periodicity (31, 33), and the absolute level of vagal-cardiac motoneuron firing is proportional to the level of respiratory sinus arrhythmia (30, 32). Moreover, in humans, large dose atropine almost completely eliminates respiratory sinus arrhythmia (18, 47). However, our results challenge the notion that respiratory sinus arrhythmia is mediated exclusively by vagal mechanisms. They suggest that sympathetic nerve activity opposes vagally mediated R-R interval oscillations and that this influence is exerted over high as well as low breathing frequencies.

It is accepted that sympathetic nerve activity influences sinoatrial node responses to vagus nerve traffic. It is arguable, however, how this interaction plays out. Some studies (48, 49) suggest that sympathetic nerve activity enhances vagal inhibition (48), an interaction Levy (37) described as "accentuated antagonism." Other studies (21), however, suggest that the opposite is true: cardiac sympathetic stimulation reduces vagally mediated heart period oscillations. Our findings support the second view but do not indicate the precise mechanism responsible for the sympathetic opposition to vagal-cardiac nerve fluctuations that we document.

We considered several possibilities. First, β-adrenergic blockade may increase arterial baroreceptor firing. This is unlikely, but not impossible. In our study, the natural baroreceptor stimulus, the arterial pressure, was insignificantly lower after than before β-adrenergic blockade (see Table 1). Moreover, in animals, β-adrenergic blockade reduces, rather than enhances, baroreceptor firing and presumably reduces sensitivity to pressure changes (11). However, we cannot totally exclude increases of phasic baroreceptor firing in our study, because with the increasing tidal breathing protocol β-adrenergic blockade increased systolic pressure spectral power (significantly at higher breathing frequencies). Second, β-adrenergic blockade may have increased vagal-cardiac motoneuron activity. To minimize this possibility, we used a hydrophilic β-adrenergic blocking drug, atenolol (40), which does not cross the blood brain barrier nearly as readily as lipophilic β-adrenergic blocking drugs, such as propranolol and metoprolol (28).

Third, sympathetic opposition to vagal-cardiac nerve activity may have occurred at the sinoatrial node. Several studies indicate that electrical sympathetic-cardiac nerve stimulation reduces responses to electrical vagus nerve stimulation (21, 45). One mechanism responsible for this effect appears to be release of the cotransmitter neuropeptide Y from sympathetic nerve endings (45). Although our results do not exclude this mechanism, they indicate that sympathetic opposition to vagal influences is not due exclusively to neuropeptide Y. The effects of neuropeptide Y are not altered by β-adrenergic blockade (35). Fourth, β-adrenergic blockade may have augmented vagal oscillations simply by lengthening R-R intervals. Sinus node susceptibility to vagal inhibition is not uniform throughout the cardiac cycle; rather, there is an optimal timing for inhibition to occur (15, 53). In our study, β-adrenergic blockade may have shifted the timing of phasic acetylcholine release into a more favorable position in the cardiac cycle (15, 55). Whatever the mechanism, our observations suggest that sympathetic nerve activity may modulate respiratory sinus arrhythmia as profoundly as vagal-cardiac nerve activity.

Previous work (52), which investigated respiratory sinus arrhythmia by widening the frequency input with random, broad-band breathing, suggested that changes in respiratory sinus arrhythmia from supine to upright posture can be partially explained by greater sympathetic modulation. This hypothesis was subsequently refined into a more comprehensive model based on pharmacological blockade (51) as in the present experiments. Although the previous model suggested both vagal and sympathetic outflows interact to generate respiratory sinus arrhythmia, the sympathetic role was defined as augmentation of heart period oscillations selectively at lower frequencies ($<$0.10 Hz). In contrast, our results suggest sympathetic restraint of heart period oscillations at all frequencies. A key difference may be that the previous work was based on heart rate, not R-R interval fluctuations during supine β-adrenergic blockade and upright cholinergic blockade. R-R interval is most closely related to cardiac vagal and sympathetic outflows (32), and heart rate is a negative curvilinear function of R-R interval. As a result, heart period variance based on heart rate in the earlier study was only two-thirds less under sympathetic conditions (atropine, upright) compared with vagal conditions (propranolol, supine), whereas estimated heart period variance based on R-R interval appears reduced by 98% under sympathetic conditions. Thus transfer function estimates based on heart rate may not accurately represent cardiac autonomic effects and should be interpreted with caution.

Atrial stretch and respiratory sinus arrhythmia. In animals, respiration-related atrial stretch generates only modest fluctuations of sinoatrial node rate (43). In heart transplant patients, whose donor sinoatrial nodes are denervated, respiratory sinus arrhythmia is unmeasurable (50) or exceedingly small (5, 25). Although the rate of atrial flutter in humans can be lessened by reductions of cardiac preload and atrial stretch (59), this effect also is small: no more than ~25 ms. These observations support the view that atrial stretch does not contribute importantly to human respiratory sinus arrhythmia.

We did not measure atrial dimensions in our study but assumed that R-R interval fluctuations after combined autonomic blockade are secondary to phasic atrial stretch. If this inference is correct, our data point toward a substantial effect of atrial stretch on R-R interval variability in humans: slow deep breathing provoked average R-R interval oscillations of ~120 ms after double autonomic blockade. Others have also found heart period oscillations persist after autonomic blockade but indicate that amplitude increases with increasing breathing frequency (51). Our findings also suggest atrial stretch can generate significant sinus arrhythmia, but only at the lowest breathing frequencies. If this effect remains in the absence of autonomic blockade, it would account for as much as 20% of respiratory sinus arrhythmia. Interestingly, the effect of respiratory-related atrial stretch on R-R intervals was less during constant tidal breathing at most frequencies. This may indicate that the human sinus node is responsive not only to the magnitude, but also to the rate of stretch, and can become refractory to the effects of stretch (26, 42). Nonetheless, our data indicate that atrial stretch can generate large R-R interval fluctuations, and may contribute importantly to respiratory sinus arrhythmia.

Effects of tidal volume on respiratory sinus arrhythmia. We found that breathing with a constant large tidal volume exerted profound influences on respiratory sinus arrhythmia. Both driving force from the model and respiratory sinus arrhythmia at higher frequencies were augmented by constant tidal breathing before autonomic blockade, to levels as great or greater than after β-blockade alone. These increases likely derive from greater blood pressure oscillations, especially at high breathing frequencies, and resultant increases of baroreflex-mediated phasic vagal outflow. Mean vagal outflow was probably unchanged because mean R-R interval was similar. Kollai and Mizsei (34) reported that in quietly breathing humans, the level of cardiac vagal activity is not zero during inspiration, and is related to the excitatory stimulation during expiration. Thus greater arterial pressure excursions with larger tidal breathing should produce concomitantly lower inspiratory and greater expiratory baroreflex-mediated vagal outflow.

Our findings further indicate that at a given mean level of vagal outflow, there is a maximal respiratory sinus arrhythmia. With constant large tidal breathing during sympathetic blockade (see Fig. 3*B*), the damping component of the respiratory sinus arrhythmia model was increased dramatically, presumably limiting the effect of high driving force on the model fit. Furthermore, average and maximal respiratory sinus arrhythmia was close to that during sympathetic blockade during increasing tidal breathing (~230 and ~370 ms). Thus large tidal breathing may produce phasic vagal outflow, which ranges from zero to maximal for the prevailing state, and this effect may not be enhanced by removal of sympathetic restraint of respiratory sinus arrhythmia.

Limitations. We blocked β-adrenergic stimulation with a dose of atenolol (0.2 mg/kg) that was worked out for propranolol (27). However, we clearly blocked β-adrenergic activity and reduced cardiac sympathetic effects. We borrowed a mathematical model from the engineering literature and attempted to explain the physiology we studied. Although this model fit our data very well, we do not identify physiological correlates for the damped oscillator model parameters. For example, driving force could be considered the sum of effectors causing respiratory sinus arrhythmia: vagal and sympathetic neural outflows, mechanical stretch, and neurohormonal modulators. However, this parameter merely provided a means of testing if sympathetic effects are focused on the resonant frequency or are spread across the range of frequencies we studied. Thus the model does not derive directly from the physiology; it merely describes the oscillations with simple parameters for ease of interpretation. Although our protocol allowed estimation of respiratory sinus arrhythmia spectral power, it was insufficient to examine relations among variables in the frequency domain. For example, by using a previously published calculation (57), the confidence interval for coherence estimates from our data would be so large that a value near unity, 0.90, would be necessary to be certain that coherence between any two signals exceeds 0 at $\alpha = 0.10$. Cross-spectral phase and magnitude estimates would suffer similarly and would likely diverge widely from one breathing frequency to the next.

Implications. It is incredibly difficult to assess cardiac autonomic drive either in animals or in humans. Thus the suggestion that a widely used vagal index is not reliable is both confounding for past studies and disconcerting for future studies. Our data in young healthy subjects during 40° head-up tilt clearly indicate that suppression of respiratory sinus arrhythmia by sympathetic effects on the sinoatrial node can be substantial. For example, respiratory sinus arrhythmia during standard frequency (0.25 Hz) and normal tidal breathing was reduced by ~56% when cardiac sympathetic outflow was intact. This has obvious implications for estimating vagal outflow in humans, but perhaps more troubling is the wide intersubject variability of this sympathetic effect. Sympathetic restraint of vagally mediated respiratory sinus arrhythmia ranged from virtually none at all to >90% during standard-frequency normal tidal breathing. This heterogenous sympathetic effect in a seemingly homoge-

nous group demonstrates the difficulty in interpreting the amplitude of respiratory sinus arrhythmia.

Despite physiological studies (20, 21, 34) questioning respiratory sinus arrhythmia as a valid and reliable cardiac parasympathetic index, this cardiovascular variability is accepted as a convenient tool for estimating the level of vagal-cardiac nerve activity. Recent committee reports (7, 56) on heart rate variability methods and interpretation have underscored a purely vagal origin for respiratory sinus arrhythmia, further reifying this variability as an acceptable measure of cardiac parasympathetic tone. Thus the routine use of respiratory sinus arrhythmia to estimate cardiac vagal outflow in physiological and pathophysiological conditions continues unabated (29, 36, 41, 58). However, our findings suggest that interpretation of respiratory sinus arrhythmia amplitude without regard to state and trait differences in cardiac sympathetic outflow are likely to lead to spurious conclusions about levels of cardiac vagal tone.

We thank Jeffrey B. Hoag for help with data analysis and Michael A. Cohen for thoughtful comments on and review of this work.

This study was supported by grants and contracts from the Department of Veterans Affairs; National Heart, Lung, and Blood Institute Grants HL-30506, HL-22296, and HL-07556; and National Aeronautics and Space Administration Grants NAG-2-408 and NAS-17720.

Present address of J. A. Taylor: Laboratory for Cardiovascular Research, Hebrew Rehabilitation Center for the Aged, 1200 Centre St., Boston, MA 02131.

REFERENCES

1. **Airaksinen KE, Ikaheimo MJ, Linnaluoto MK, Niemela M, and Takkunen JT.** Impaired vagal heart rate control in coronary artery disease. *Br Heart J* 58: 592–597, 1987.
2. **Angelone A and Coulter N.** Respiratory sinus arrhythmia: a frequency-dependent phenomenon. *J Appl Physiol* 19: 479–482, 1964.
3. **Baskerville AL, Eckberg DL, and Thompson MA.** Arterial pressure and pulse interval responses to repetitive carotid baroreceptor stimuli in man. *J Physiol (Lond)* 297: 61–71, 1979.
4. **Berger R, Saul JP, and RJ C.** Transfer function analysis of autonomic regulation. I. Canine atrial rate response. *Am J Physiol Heart Circ Physiol* 256: H142–H152, 1989.
5. **Bernardi L, Keller F, Sanders M, Reddy PS, Griffith B, Meno F, and Pinsky MR.** Respiratory sinus arrhythmia in the denervated human heart. *J Appl Physiol* 67: 1447–1455, 1989.
7. **Berntson GG, Bigger JT Jr, Eckberg DL, Grossman P, Kaufmann PG, Malik M, Nagaraja HN, Porges SW, Saul JP, Stone PH, and van der Molen MW.** Heart rate variability: origins, methods, and interpretive caveats. *Psychophysiology* 34: 623–648, 1997.
8. **Brown TE, Beightol LA, Koh J, and Eckberg DL.** Important influence of respiration on human R-R interval power spectra is largely ignored. *J Appl Physiol* 75: 2310–2307, 1993.
9. **Comroe J, Forster H, Dubois A, Briscoe W, and Carlsen E.** *The Lung. Clinical Physiology and Pulmonary Function Tests*. Chicago, IL: Year Book, 1962.
10. **Cooke WH, Cox JF, Diedrich AM, Taylor JA, Beightol LA, Ames JET, Hoag JB, Seidel H, and Eckberg DL.** Controlled breathing protocols probe human autonomic cardiovascular rhythms. *Am J Physiol Heart Circ Physiol* 274: H709–H718, 1998.
11. **Dorward PK and Korner PI.** Effect of *d*,*l*-propranolol on renal sympathetic baroreflex properties and aortic baroreceptor activity. *Eur J Pharmacol* 52: 61–71, 1978.
12. **Drummond PD.** Parasympathetic cardiac control in mild hypertension. *J Hypertens* 8: 383–387, 1990.
13. **Eckberg DL.** Human sinus arrhythmia as an index of vagal cardiac outflow. *J Appl Physiol* 54: 961–966, 1983.
14. **Eckberg DL.** Nonlinearities of the human carotid baroreceptor-cardiac reflex. *Circ Res* 47: 208–216, 1980.
15. **Eckberg DL, Abboud FM, and Mark AL.** Modulation of carotid baroreflex responsiveness in man: effects of posture and propranolol. *J Appl Physiol* 41: 383–387, 1976.
16. **Eckberg DL and Eckberg MJ.** Human sinus node responses to repetitive, ramped carotid baroreceptor stimuli. *Am J Physiol Heart Circ Physiol* 242: H638–H644, 1982.
17. **Eckberg DL, Kifle YT, and Roberts VL.** Phase relationship between normal human respiration and baroreflex responsiveness. *J Physiol (Lond)* 304: 489–502, 1980.
18. **Fouad FM, Tarazi RC, Ferrario CM, Fighaly S, and Alicandri C.** Assessment of parasympathetic control of heart rate by a noninvasive method. *Am J Physiol Heart Circ Physiol* 246: H838–H842, 1984.
19. **Fredericq L.** De l'influence de la respiration sur la circulation. *Arch Biol* 3: 55–100, 1887.
20. **Hedman AE, Hartikainen JE, Tahvanainen KU, and Hakumaki MO.** The high frequency component of heart rate variability reflects cardiac parasympathetic modulation rather than parasympathetic tone. *Acta Physiol Scand* 155: 267–273, 1995.
21. **Hedman AE, Tahvanainen KU, Hartikainen JE, and Hakumaki MO.** Effect of sympathetic modulation and sympathovagal interaction on heart rate variability in anaesthetized dogs. *Acta Physiol Scand* 155: 205–214, 1995.
22. **Henry RA, Lu IL, Beightol LA, and Eckberg DL.** Interactions between CO2 chemoreflexes and arterial baroreflexes. *Am J Physiol Heart Circ Physiol* 274: H2177–H2187, 1998.
23. **Hill-Smith I and Purves RD.** Synaptic delay in the heart: an ionophoretic study. *J Physiol (Lond)* 279: 31–54, 1978.
24. **Hirsch JA and Bishop B.** Respiratory sinus arrhythmia in humans: how breathing pattern modulates heart rate. *Am J Physiol Heart Circ Physiol* 241: H620–H629, 1981.
25. **Hrushesky WJ, Fader D, Schmitt O, and Gilbertsen V.** The respiratory sinus arrhythmia: a measure of cardiac age. *Science* 224: 1001–1004, 1984.
26. **James TN.** The sinus node as a servomechanism. *Circ Res* 32: 307–313, 1973.
27. **Jose A and Taylor RR.** Autonomic blockade by propranolol and atropine to study intrinsic myocardial function in man. *J Clin Invest* 48: 2019–2031, 1969.
28. **Kaila T and Marttila R.** Receptor occupancy in lumbar CSF as a measure of the antagonist activity of atenolol, metoprolol and propranolol in the CNS. *Br J Clin Pharmacol* 35: 507–515, 1993.
29. **Kardos A, Long V, Bryant J, Singh J, Sleight P, and Casadei B.** Lipophilic versus hydrophilic beta(1) blockers and the cardiac sympathovagal balance during stress and daily activity in patients after acute myocardial infarction. *Heart* 79: 153–160, 1998.
30. **Katona PG and Jih F.** Respiratory sinus arrhythmia: noninvasive measure of parasympathetic cardiac control. *J Appl Physiol* 39: 801–805, 1975.
31. **Katona PG, Poitras JW, Barnett GO, and Terry BS.** Cardiac vagal efferent activity and heart period in the carotid sinus reflex. *Am J Physiol* 218: 1030–1037, 1970.
32. **Koizumi K, Terui N, and Kollai M.** Effect of cardiac vagal and sympathetic nerve activity on heart rate in rhythmic fluctuations. *J Auton Nerv Syst* 12: 251–259, 1985.
33. **Kollai M and Koizumi K.** Reciprocal and non-reciprocal action of the vagal and sympathetic nerves innervating the heart. *J Auton Nerv Syst* 1: 33–52, 1979.
34. **Kollai M and Mizsei G.** Respiratory sinus arrhythmia is a limited measure of cardiac parasympathetic control in man. *J Physiol (Lond)* 424: 329–342, 1990.
35. **Koyanagawa H, Musha T, Kanda A, Kimura T, and Satoh S.** Inhibition of vagal transmission by cardiac sympathetic nerve stimulation in the dog: possible involvement of opioid receptor. *J Pharmacol Exp Ther* 250: 1092–1096, 1989.
36. **Kuo CD and Chen GY.** Comparison of three recumbent positions on vagal and sympathetic modulation using spectral heart rate variability in patients with coronary artery disease. *Am J Cardiol* 81: 392–396, 1998.

37. **Levy MN.** Sympathetic-parasympathetic interactions in the heart. *Circ Res* 29: 437–445, 1971.
38. **Lopes OU and Palmer JF.** Proposed respiratory 'gating' mechanism for cardiac slowing. *Nature* 264: 454–456, 1976.
39. **Moriguchi A, Otsuka A, Kohara K, Mikami H, and Ogihara T.** Evaluation of orthostatic hypotension using power spectral analysis. *Am J Hypertens* 6: 198–203, 1993.
40. **Neil-Dwyer G, Bartlett J, McAinsh J, and Cruickshank JM.** Beta-adrenoceptor blockers and the blood-brain barrier. *Br J Clin Pharmacol* 11: 549–553, 1981.
41. **Osterhues HH, Grossmann G, Kochs M, and Hombach V.** Heart-rate variability for discrimination of different types of neuropathy in patients with insulin-dependent diabetes mellitus. *J Endocrinol Invest* 21: 24–30, 1998.
42. **Pathak CL.** Autoregulation of chronotropic response of the heart through pacemaker stretch. *Cardiology* 58: 45–64, 1973.
43. **Perlini S, Solda PL, Piepoli M, Sala-Gallini G, Calciati A, Finardi G, and Bernardi L.** Determinants of respiratory sinus arrhythmia in the vagotomized rabbit. *Am J Physiol Heart Circ Physiol* 269: H909–H915, 1995.
44. **Porter TR, Eckberg DL, Fritsch JM, Rea RF, Beightol LA, Schmedtje JF Jr, and Mohanty PK.** Autonomic pathophysiology in heart failure patients. Sympathetic-cholinergic interrelations. *J Clin Invest* 85: 1362–1371, 1990.
45. **Potter EK.** Prolonged non-adrenergic inhibition of cardiac vagal action following sympathetic stimulation: neuromodulation by neuropeptide Y? *Neurosci Lett* 54: 117–121, 1985.
46. **Press WH, Flannery BP, Teukolsky SA, and Vetterling WT.** *Numerical Recipes in Pascal: The Art of Scientific Computing*. Cambridge, UK: Cambridge Univ. Press, 1989.
47. **Raczkowska M, Eckberg DL, and Ebert TJ.** Muscarinic cholinergic receptors modulate vagal cardiac responses in man. *J Auton Nerv Syst* 7: 271–278, 1983.
48. **Rosenbluth A and Simeone F.** The interrelations of vagal and accelerator effects on the cardiac rate. *Am J Physiol* 110: 42–55, 1935.
49. **Samaan A.** The antagonistic cardiac nerves and heart rate. *J Physiol (Lond)* 83: 332–340, 1935.
50. **Sands KE, Appel ML, Lilly LS, Schoen FJ, Mudge GH Jr, and Cohen RJ.** Power spectrum analysis of heart rate variability in human cardiac transplant recipients. *Circulation* 79: 76–82, 1989.
51. **Saul JP, Berger RD, Albrecht P, Stein SP, Chen MH, and Cohen RJ.** Transfer function analysis of the circulation: unique insights into cardiovascular regulation. *Am J Physiol Heart Circ Physiol* 261: H1231–H1245, 1991.
52. **Saul JP, Berger RD, Chen MH, and Cohen RJ.** Transfer function analysis of autonomic regulation. II. Respiratory sinus arrhythmia. *Am J Physiol Heart Circ Physiol* 256: H153–H161, 1989.
53. **Seidel H, Herzel H, and Eckberg DL.** Phase dependencies of the human baroreceptor reflex. *Am J Physiol Heart Circ Physiol* 272: H2040–H2053, 1997.
54. **Spear JF, Kronhaus KD, Moore EN, and Kline RP.** The effect of brief vagal stimulation on the isolated rabbit sinus node. *Circ Res* 44: 75–88, 1979.
55. **Stuesse SL, Wallick DW, Zieske H, and Levy MN.** Changes in vagal phasic chronotropic responses with sympathetic stimulation in the dog. *Am J Physiol Heart Circ Physiol* 241: H850–H856, 1981.
56. **Task Force of the European Society of Cardiology and the North American Society of Pacing and Electrophysiology.** Heart rate variability. Standards of measurement, physiological interpretation, and clinical use. *Eur Heart J* 17: 354–381, 1996.
57. **Taylor JA, Carr DL, Myers CW, and Eckberg DL.** Mechanisms underlying very-low-frequency RR-interval oscillations in humans. *Circulation* 98: 547–555, 1998.
58. **Vesalainen RK, Kantola IM, Airaksinen KE, Tahvanainen KU, and Kaila TJ.** Vagal cardiac activity in essential hypertension: the effects of metoprolol and ramipril. *Am J Hypertens* 11: 649–658, 1998.
59. **Wallin BG, Esler M, Dorward P, Eisenhofer G, Ferrier C, Westerman R, and Jennings G.** Simultaneous measurements of cardiac noradrenaline spillover and sympathetic outflow to skeletal muscle in humans. *J Physiol (Lond)* 453: 45–58, 1992.
60. **Waxman MB, Yao L, Cameron DA, and Kirsh JA.** Effects of posture, Valsalva maneuver and respiration on atrial flutter rate: an effect mediated through cardiac volume. *J Am Coll Cardiol* 17: 1545–1552, 1991.
61. **Welch PD.** The use of fast Fourier transform for the estimation of power spectra: a method based on time averaging over short, modified periodograms. *IEEE Trans Audio Electroacoust* 15: 70–73, 1967.
62. **Womack BF.** The analysis of respiratory sinus arrhythmia using spectral analysis and digital filtering. *IEEE Trans Biomed Eng* 18: 399–499, 1971.